doi: 10.4149/gpb_2024049

Hsa_circ_0007905 as a modulator of miR-330-5p and VDAC1: Enhancing stemness and reducing apoptosis in cervical cancer stem cells

JianPing Zheng[1], Yan Feng[1] and ChaoYan Yuan[1]

[1] *Department of Gynaecology, Minda Hospital Affiliated to Hubei Minzu University, Enshi City, Hubei Province, China*

Abstract. Circular RNAs (circRNAs) are covalently closed RNA structures that play a pivotal role in the initiation and progression of cervical cancer (CC). However, it is unclear how these RNAs influence cancer stem cell (CSC)-like properties in CC. Here, we performed circRNA microarray analysis and identified an intergenic circRNA, hsa_circ_0007905, that was significantly upregulated in patients with CC. Moreover, hsa_circ_0007905 was found to be highly expressed in CSC-enriched subsets of cervical cancer cell lines. Functionally, knocking down hsa_circ_0007905 suppressed proliferative, migratory invasive and self-renewal abilities, as well as stimulated apoptosis of CSCs in CC. Mechanistically, hsa_circ_0007905 functions as a "sponge" to inversely control miR-330-5p expression, which directly targets VDAC1. Overexpressing VDAC1 or inhibiting miR-330-5p blocked the roles of silencing hsa_circ_0007905 on CSCs. Thus, we revealed the mechanism by which hsa_circ_0007905 competitively adsorbs miR-330-5p to mediate VDAC1 expression to promote stemness and inhibit apoptosis of CSCs in CC, offering an therapeutic target for treating CC.

Key words: Cervical cancer stem cells — hsa_circ_0007905 — miR-330-5p — VDAC1 — Apoptosis

Introduction

In global terms, cervical cancer (CC) is the fourth most common cancer among women (Mailinh et al. 2018; Buskwofie et al. 2020; Hyuna et al. 2021). China reportedly accounted for 11.9% of global CC deaths and 12.3% of CC disability-adjusted life-years in 2017 (Guo et al. 2021), and the incidence of CC has shown a trend toward younger age (Bray et al. 2018). While the incidence and mortality rates of CC have decreased worldwide due to CC screening and human papillomavirus (HPV) vaccination (Brisson et al. 2020), the threat posed by CC still cannot be ignored. In patients with early-stage CC, standardized treatment and management can be helpful (Koh et al. 2019; Ferrall et al. 2021), but advanced and metastatic CC miss the optimal treatment window and have limited treatment efficacy, which results in a significantly lower 5-year survival rate (Wang et al. 2019). Recent studies suggest that CC recurrences and metastases may be related to cervical cancer stem cells (CSCs), or that stem cells act as seed cells for the cancer (Yao et al. 2015; Di Fiore et al. 2022). The discovery of the mechanism by which CC CSCs develop is therefore of great importance to providing more effective treatments for advanced, recurrent and drug-resistant patients.

Circular RNA (circRNA) is an endogenous non-coding RNA, which is widely present in various eukaryotic cells. circRNA has a closed ring structure, which is not easily degraded by exonuclease and ribonuclease. circRNAs, as sponge molecules of miRNAs, reduce the ability of miRNAs to target mRNA, and participate in the regulation of physiological functions of cells (Chen S et al. 2021). CircRNAs are abnormally expressed in multiple tumors (Chen and Shan 2021). In CC, circ_400029 (Ma et al. 2022), circ_0087429 (Yang et al. 2022) and hsa_circ_101996 (16) reduce the ability of miRNAs to target mRNA, thereby regulating

Electronic supplementary material. The online version of this article (doi: 10.4149/gpb_2024049) contains Supplementary material.

Correspondence to: ChaoYan Yuan, Department of Gynaecology, Minda Hospital Affiliated to Hubei Minzu University, No. 2 Wufengshan Road, Enshi City, Hubei Province, 445000, China
E-mail: yuanchaoydl88df@outlook.com

the biological behavior of CC cells. circ_000448 is highly expressed in CC cell subsets rich in CSCs and can induce CSC-like characteristics.

Hsa_circ_0007905 is a circRNA derived from the STX6 gene, also known as circSTX6. In pancreatic cancer (Meng et al. 2022), hepatocellular carcinoma (Lu et al. 2023) and bladder cancer (Wei et al. 2024), hsa_circ_0007905 is a cancer-promoting factor that is associated with drug resistance. We confirmed the abnormal expression of hsa_circ_0007905 in CC by GEO database analysis and RT-qPCR detection and explored the mechanism of hsa_circ_0007905 involved in CC stemness.

Materials and Methods

Bioinformatics analysis

We obtained open access RNA expression profiles and corresponding information from the GSE102686 project of the NCBI GEO database. We extracted RNA expression profiles from 5 CC tissue samples and 5 adjacent normal tissue samples, and the annotation platform is GPL19978. The differential genes in the GSE102686 database were analyzed by R language software. Genes with Log2 Fold change > 1 and $p < 0.05$ were labeled as differential genes.

Participants and tissue collection

From January 2019 to October 2023, 53 cases of CC tissues and their corresponding adjacent tissues were collected from Minda Hospital Affiliated to Hubei Minzu University. Pathological examination confirmed that no residual cancer cells were present in the adjacent tissues that were at least 5 cm away from the edge of the tumor. Upon resection, the tissues were frozen in liquid nitrogen and stored at −80°C.

Case inclusion criteria: (1) CC was confirmed by cervical biopsy, cervical smears, colposcopy, cervical iodine test, and cervical resection; (2) There was no treatment such as radiotherapy and chemotherapy 2 weeks before surgery.

Case exclusion criteria: (1) History of radiotherapy or chemotherapy; (2) Object to sample collection; (3) Immune system diseases.

All subjects signed informed consent for this study, and this study was approved by Minda Hospital Affiliated to Hubei Minzu University ethics committee. All included patients are depicted in Table 1 according to their clinicopathological characteristics.

Cell culture

Non-cancerous cervical epithelial cell line Ect1/E6E7 and human CC cell lines SiHa, HeLa, and CaSki (ATCC, Manassas, VA, USA) were cultured in DMEM containing 10% fetal bovine serum, 100 μg/ml penicillin and 100 μg/ml streptomycin (Bioctyocare, Guangzhou, China) at 37°C, 5% CO_2, digested and passaged every 2–3 days.

After RT-qPCR was conducted, the cell line with the largest difference in hsa_circ_0007905 expression from Ect1/E6E7 was tested for subsequent experiments.

RNase R assay

The total RNA of CaSki cells was extracted and digested with RNase R (3 U/μg RNA, Geneseed, Guangzhou, China) at 37°C for 30 min. RNA was purified using RNeasy MinElute

Table 1. The correlation between the expression level of hsa_circ_0007905 and the clinicopathological features of cervical cancer

Clinical pathology parameters	Cases ($n = 53$)	hsa_circ_0007905		p
		low expression ($n = 27$)	high expression ($n = 26$)	
Age				0.865
≤ 45 years	21	11	10	
> 45 years	32	16	16	
Tumor size				0.075
≤ 4 cm	29	18	11	
> 4 cm	24	9	15	
Lymphatic metastasis				0.026
NO	38	23	15	
YES	15	4	11	
FIGO staging				0.006
Ib~IIa	36	23	13	
IIb~IIIa	17	4	13	

Cleaning Kit (Qiagen, Germantown, MD, USA). Hsa_circ_0007905 and linear STX6 were detected by RT-qPCR.

Actinomycin D assay

CaSki cells were placed in 6-well plates at 5×10^5 cells/well. Actinomycin D (Sigma) was added to each well at 2 μg/ml at 0, 4, 8, 12 and 24 h, and cells were collected at each time point to determine RNA using RT-qPCR.

Separation of nuclear and cytoplasmic fractions

Separation of the nuclear and cytoplasmic segments of CaSki cells was achieved through the use of PARIS kits (Life Technologies, CA, USA). Approximately 2×10^6 cells underwent two washes using ice PBS and were then combined with 450 μl of cell separation buffer on ice for five minutes, succeeded by a five-minute centrifugation at 4°C and 500 revolutions *per* minute. The cytoplasmic RNA and nuclear RNA were collected for RT-qPCR analysis. Nucleus and cytoplasm were referenced by U6 and GAPDH, respectively.

Sorting of CSCs

CaSki cells were digested with trypsin and adjusted to 1×10^6/ml with PBS buffer. CD133 antibody (BD Pharmagen, USA) was mixed in dark for 20 min. Flow cytometry (BD Biosciences, Bedford, MA, USA) sorted and identified $CD133^+$ CaSki cells as CaSki CSCs (Qi et al. 2014; Gao et al. 2021).

Cell transfection

The siRNAs targeting hsa_circ_0007905 (si-circ_0007905#1 and si-circ_0007905#2) (Table S1 in Supplementary material) and negative control (si-NC), as well as the plasmid overexpressing VDAC1 (pcDNA3.1-VDAC1) and negative control (pcDNA3.1) were synthesized by KeyGEN (Nanjing, China). miR-330-5p mimics and miR-330-5p inhibitors (Table S1) and their negative controls (mimics NC and inhibitors NC) were synthesized by Ribobio (Guangzhou, China). After trypsin digestion of $CD133^+$ CaSki cells, they were inoculated into 6-well plates at 3×10^6 cells/well. Upon reaching 60% cell confluence, CSCs were moved to a serum-free environment for an hour. Subsequently, the sequence or plasmid was introduced into CSCs *via* Lipofectamine 2000 (Invitrogen, Carlsbad, CA, USA). Efficiency in transfection was measured using RT-qPCR or Western blot techniques.

RT-qPCR

TRIzol reagent (Invitrogen, Carlsbad, CA, USA) was used to extract total RNA. The RNAs were reverse transcribed using PrimeScript RT Reagent Kitt (Takara Biotechnology, Japan) in accordance with the manufacturer's specifications. In addition, miRNA reverse transcription were performed using the TaqMan™ MicroRNA reverse transcription reagents (Applied Biosystems, USA) according to the manufacturer's instructions and a stem-loop RT primer (Table 2) was used for RT of miR-330-5p. Real-time PCR testing was carried out on ABI 7500 fast PCR System (Carlsbad, CA, USA) with a SYBR green PCR Master Mix (TOYOBO, Japan). Primers listed in Table 2 were designed by Sangon biotech (Shanghai, China). The results were analyzed by relative quantitative $2^{-\Delta\Delta CT}$ method.

Western blot

Proteins from tissues and cells were isolated using RIPA lysis buffer (Beyotime, Shanghai, China), and their concentration was measured using the BCA kit (AmyJet Scientific, Hubei, China). After extraction, the protein was combined with the loading buffer, heated for 5 min, immersed in ice, and then isolated using 10% polyacrylamide gel electrophoresis. The protein underwent a transfer onto a nitrocellulose membrane, was treated with 5% skim milk in TBST for an hour, and then combined with primary antibodies VDAC1 (1:1000, ab306581; Abcam), Bax (1:1000, #5023, Cell Signaling Technology), Bcl-2 (1:500, ab196495, Abcam), CD44 (1:100, #37259, Cell Signaling Technology), SOX2 (1:1000, #14962, Cell Signaling Technology), OCT4 (1:1000, #2890, Cell Signaling Technology), and GAPDH (1:1000; ab9485, Abcam), maintained overnight at 4°C. Subsequently, the membranes underwent a triple 5-min room temperature rinse with PBS, were combined with horseradish peroxidase-tagged goat anti-rabbit IgG secondary antibody (1:5000, Abcam) for an hour, and then moved into the ECL reaction

Table 2. Primers used in RT-qPCR analysis

Genes	Sequences (5'→3')
miR-330-5p	RT: GTCGTATCCAGTGCAGGGTCCGAG GTATTCGCACTGGATACGACGCCTAA
	F: ATTATCGCTCTCTGGGCCTG
	R: TATGGTTGTAGACGACTCCTTGAC
U6	F: CTCGCTTCGGCAGCACA
	R: AACGCTTCACGAATTTGCGT
hsa_circ_0007905	F: TGGAGGAACAGGCAGTTATGTTG
	R: TTGACATCTGATCTTTCATGTCCAC
STX6	F: CTGCGGACTGTGAAGAATCA
	R: CGTGCATTCTGAAATTGTGG
VDAC1	F: ACGTATGCCGATCTTGGCAAA
	R: TCAGGCCGTACTCAGTCCA
GAPDH	F: CTGGGCTACACTGAGCACC
	R: AAGTGGTCGTTGAGGGCAATG

F, forward; R, reverse.

solution (Pierce, USA) for a minute. Subsequently, the membranes were captured using a Bio-rad Gel Doc EZ imaging device. The analysis of protein images was conducted using ImageJ2x software.

CCK-8

Cells were seeded into 96-well plates at 1×10^4 cells/well and mixed with10 μl CCK-8 solution (Beyotime) at 24, 48 and 72 h, respectively. After 1 h, the absorbance was measured at 450 nm by Multiskan Spectrum full-wavelength microplate reader.

Tumor sphere formation

The cells were inoculated in a 6-well plate containing serum-free DMEM/F12 (Gibco, NY, USA) at 2000 cells/well. The medium contained 20 ng/ml epidermal growth factor (Calbiochem, CA, USA), B27 (1:50; Invitrogen), and 0.5% bovine serum albumin (Sigma-Aldrich, St. Louis, MO, USA). After 2 weeks, the number of cell spheres (spherical non-adherent clumps with diameter > 100 μm) was counted under the Nikon Eclipse TE2000-S microscope.

Flow cytometry

The cells underwent digestion using 0.25% trypsin (without EDTA) (PYG0107, Boster, Wuhan, China) followed by centrifugation. After extracting the supernatant, the residual substance was processed through centrifugation. The Annexin-V-FITC/PI staining mixture was concocted utilizing the Annexin-V-FITC kit for detecting apoptosis (K201-100, Biovision, USA). A total of 1×10^6 cells were reconstituted in a 100 μl solution for staining and then incubated for 15 min. FITC and PI fluorescence was captured using a 488 nm excitation at 515 nm and a 620 nm bandpass filter, respectively. The apoptosis was detected by flow cytometry (BD Biosciences).

Cell scratch test

Cells were placed into a 6-well plate (3×10^5 cells/well) and left for 24 h. A sterile 200 μl tip was perpendicular to the cell plate and scratched on the cell layer. After the scratch was completed, non-adherent cells were removed, and a new medium was supplemented. At 0 and 48 h respectively, the scratch width was observed and measured under a microscope, and the percentage of scratch healing was calculated.

Transwell experiment

Cells were digested to prepare cell suspension. Each Transwell chamber (pore size 8 μm, Millpore, USA) was covered with 80 μl Matrigel diluted at 1:8 (only for invasion assay), inoculated with 1×10^5 cells, and added with 100 μl serum-free DMEM. The lower chamber was covered with complete medium. Following a 24-h period, cells in the bottom chamber underwent fixation using 4% paraformaldehyde for a quarter of an hour, followed by a 10-min crystal violet staining, and were then photographed across five different areas under a microscope.

Dual-luciferase reporter assay

The bioinformatics website was employed to examine the binding sites of hsa_circ_0007905/VDAC1 and miR-330-5p. Synthesis was performed on the miR-330-5p targeting site sequence, which includes hsa_circ_0007905/VDAC1 (WT) and the mutated sequence (MUT). To digest the pmiR-RB-REPORTTM plasmid (RiboBio, Guangzhou, China), restriction endonucleases were employed. The generated WT and MUT target sequences were incorporated into the pmiR-RB-REPORTTM vector (RiboBio). MUT and WT vectors underwent co-transfection with NC mimics and miR-330-5p mimics into the cells, respectively. After 48 h, the cells underwent lysis, a 3–5 min centrifugation, and the supernatant was collected. The detection of firefly luciferase and renilla luciferase was achieved through the application of the Beyotime luciferase detection kit (RG005).

RNA-pull down assay

Biotin-tagged miR-330-5p wild-type plasmid and biotin-tagged miR-330-5p mutant plasmid (50 nM each) (RiboBio) were used to transfect cells. Following 48 h, the cells underwent a 10-min incubation with a designated cell lysis buffer (Ambion, USA), after which the lysates were treated with M-280 streptavidin magnetic beads (Sigma) already coated with RNase-free and yeast tRNA (Sigma). Post-elution, a counteracting let-7f probe (Table S1) was established to serve as a negative control. Trizol was used to extract the total RNA, followed by the measurement of hsa_circ_0007905 and VDAC1 through RT-qPCR.

Statistical analysis

Data were processed using the GraphPad Prism 9 software. All experiments in this study were performed independently with at least five biological replicates. The data were expressed as the means ± standard deviation (SD). A t-test was employed to examine the differences between the two groups. Analyses comparing various groups were conducted using One-way ANOVA and Tukey's multiple comparisons test. To analyze correlations, Pearson's correlation coefficient was employed, and chi-square assessments were conducted on

the clinicopathological traits of CC patients. A *p*-value below 0.05 signals a difference of statistical significance.

Results

Circular RNA hsa_circ_0007905 is up-regulated in CC

Circular RNA hsa_circ_0007905 was significantly up-regulated in CC tissues from the data analysis obtained from the GSE102686 database (Fig. 1A). RT-qPCR detection presented higher hsa_circ_0007905 expression in CC tissues from enrolled patients (Fig. 1B). Based on hsa_circ_0007905 median expression, CC patients were categorized into groups with high and low expression, and the correlation between hsa_circ_0007905 and CC's clinicopathological characteristics was examined (Table 1). We found that hsa_circ_0007905 high expression in CC tissues was associated with lymph node metastasis and FIGO stage.

In addition, hsa_circ_0007905 was up-regulated in CC cell lines, especially in CaSki cells compared with Ect1/E6E7 cells (Fig. 1C). Therefore, CaSki cells were selected to verify the characteristics and location of hsa_circ_0007905. In contrast to linear STX6, hsa_circ_0007905 showed resistance to treatment with RNase R and actinomycin D, confirming the stability of hsa_circ_0007905 (Fig. 1D,E). Meanwhile, hsa_circ_0007905 was confirmed to be mainly expressed in the cytoplasm (Fig. 1F).

Silencing hsa_circ_0007905 inhibits the stemness of CSCs and promotes apoptosis

CaSki cells were sorted by flow cytometry. The percentage of $CD133^+$ in CaSki cells after sorting was higher, and CSC markers CD44, OCT4 and SOX2 were also significantly up-regulated, indicating that CSCs were successfully sorted (Fig. 2A,B). Hsa_circ_0007905 in $CD133^+$ CaSki cells and CasKi cells was detected by RT-qPCR. Hsa_circ_0007905 level in $CD133^+$ CaSki cells was higher, suggesting that hsa_circ_0007905 may be related to the stemness of CC cells (Fig. 2C). To further study the effect of hsa_circ_0007905 on CSCs, we transfected siRNA targeting hsa_circ_0007905 (si-circ_0007905#1 and si-circ_0007905#2) into $CD133^+$ CaSki cells. RT-qPCR verified that si-circ_0007905#1 and si-circ_0007905#2 successfully changed hsa_circ_0007905 expression in cells (Fig. 2D). CCK-8 test revealed that hsa_circ_0007905 downregulation curtailed the proliferation of $CD133^+$ CaSki cells (Fig. 2E). Flow cytometry and Western blot experiments showed that low expression of hsa_circ_0007905 increased the apoptosis rate and Bax, and inhibited Bcl-2 (Fig. 2F,G). The sphere formation experiment manifested that after silencing hsa_circ_0007905, the num-

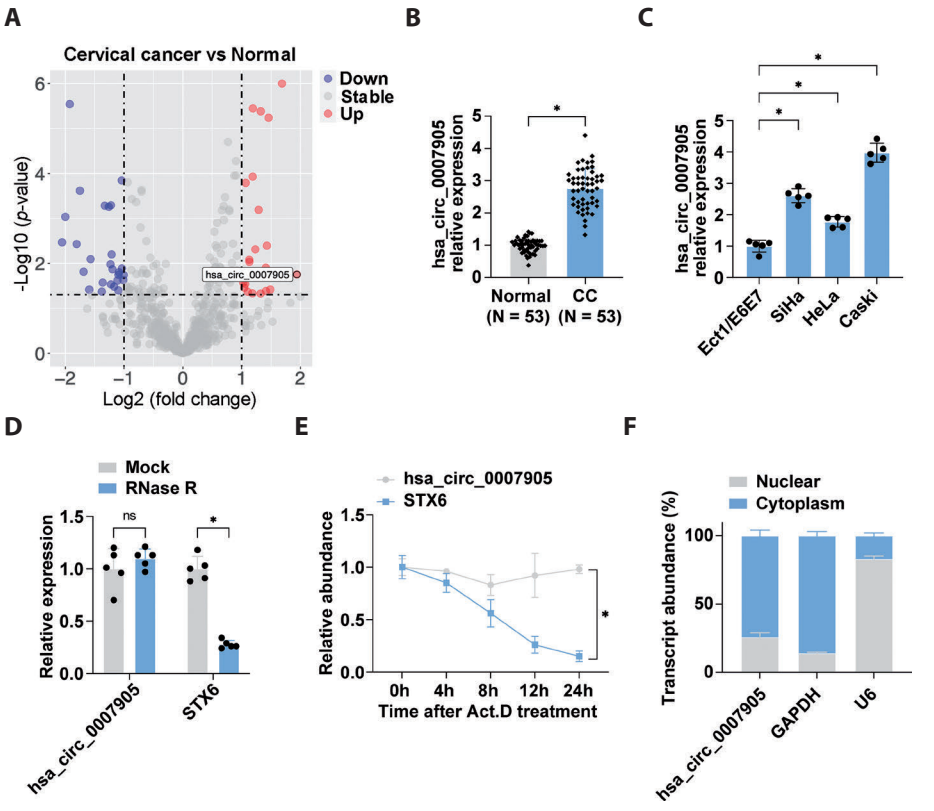

Figure 1. Up-regulation of hsa_circ_0007905 in CC. **A.** Volcano map of differential expression of circRNAs in CC tissues and adjacent tissues (in the GSE102686 dataset). **B.** RT-qPCR to detect the expression of hsa_circ_0007905 in CC tissues and adjacent tissues (n = 53). **C.** RT-qPCR to detect the expression of hsa_circ_0007905 in Ect1/E6E7 and human CC cell lines SiHa, HeLa and CaSki. **D.** RT-qPCR to detect the expression of hsa_circ_0007905 and STX6 after RNaseR treatment. **E.** RT-qPCR to detect the expression of hsa_circ_0007905 and STX6 after actinomycin D treatment. **F.** Nuclear and cytoplasmic separation experiment to detect relative expression of hsa_circ_0007905 in cytoplasm and nucleus. * $p < 0.05$.

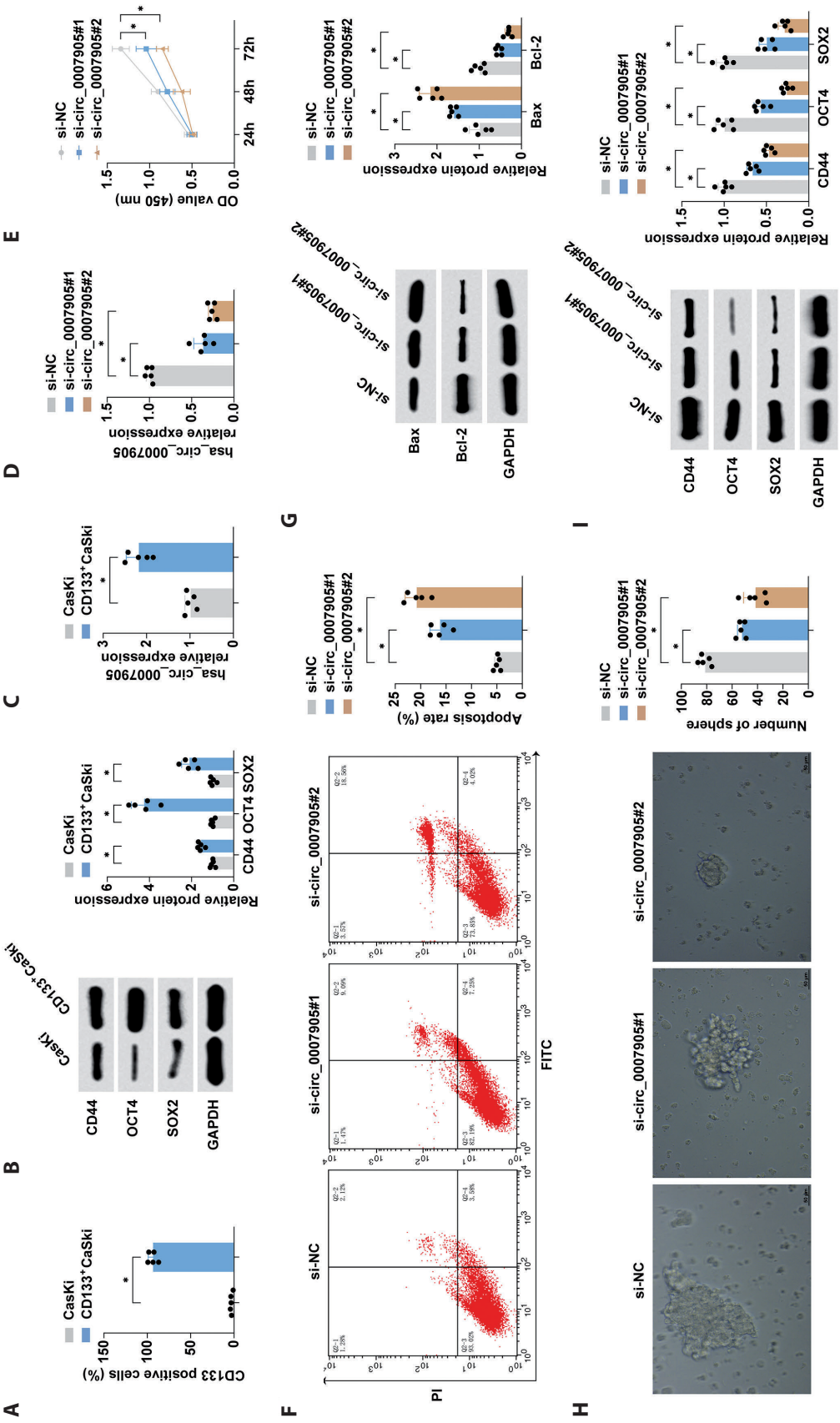
A
CD133 positive cells (%)
CasKi
CD133+CaSki
B
CD44
OCT4
SOX2
GAPDH
Relative protein expression
CD44 OCT4 SOX2
C
hsa_circ_0007905 relative expression
D
hsa_circ_0007905 relative expression
si-NC
si-circ_0007905#1
si-circ_0007905#2
E
OD value (450 nm)
24h
48h
72h
F
si-NC
si-circ_0007905#1
si-circ_0007905#2
PI
FITC
G
Apoptosis rate (%)
si-NC
si-circ_0007905#1
si-circ_0007905#2
si-NC
si-circ_0007905#1
si-circ_0007905#2
Bax
Bcl-2
GAPDH
Relative protein expression
H
si-NC
si-circ_0007905#1
si-circ_0007905#2
I
Number of sphere
si-NC
si-circ_0007905#1
si-circ_0007905#2
si-NC
si-circ_0007905#1
si-circ_0007905#2
CD44
OCT4
SOX2
GAPDH
Relative protein expression
CD44
OCT4
SOX2

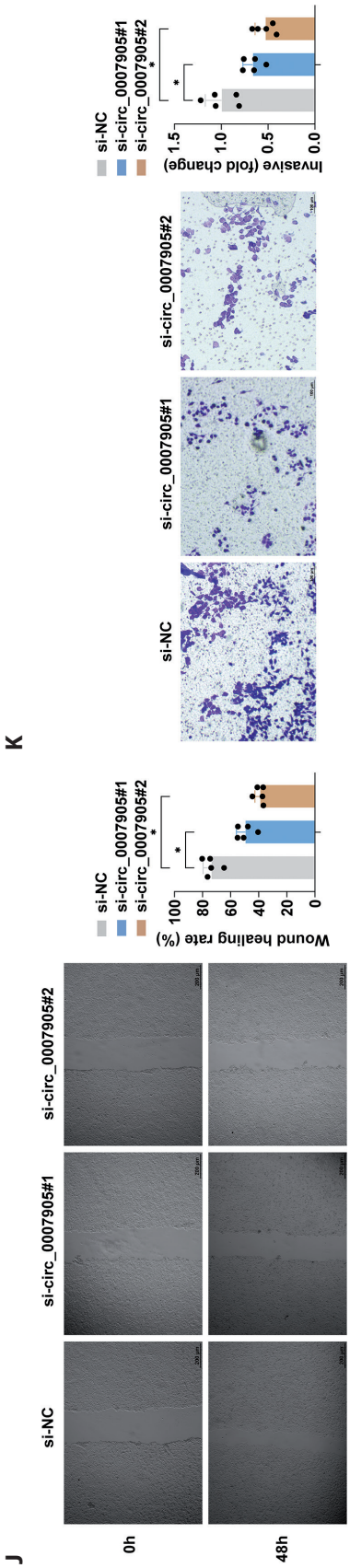

Figure 2. Silencing hsa_circ_0007905 inhibits the stemness of CSCs and promotes apoptosis. **A.** The proportion of $CD133^+$ CaSki cells before and after flow cytometry sorting. **B.** Western blot to detect the protein expression of CD44, OCT4 and SOX2 before and after sorting. **C.** RT-qPCR to detect the expression of hsa_circ_0007905 in $CD133^+$ CaSki cells and CasKi cells. **D.** RT-qPCR to detect the expression of hsa_circ_0007905 in $CD133^+$ CaSki cells after transfection. **E.** CCK-8 assay to detect cell proliferation. **F.** Flow cytometry to detect apoptosis. **G.** Western blot to detect the protein expression of Bax and Bcl-2. **H.** Sphere formation assay to detect the number of spheres. **I.** Western blot to detect the protein expression of CD44, OCT4 and SOX2. **J.** Scratch test to detect cell migration in each group. **K.** Transwell to detect cell invasion. * $p < 0.05$.

ber of spheres formed by $CD133^+$ CaSki cells was significantly reduced, suggesting that the self-renewal ability of cells was weakened and the stemness of cells was inhibited (Fig. 2H). Also, silencing hsa_circ_0007905 inhibited CD44, OCT4 and SOX2 protein expression (Fig. 2I). Scratch test results showed that the scratch healing rate and migration ability of cells decreased after low expression of hsa_circ_0007905 (Fig. 2J). Cell invasion was inhibited by hsa_circ_0007905 downregulation in transwell experiments (Fig. 2K).

Hsa_circ_0007905 competitively targets miR-330-5p

After confirming the effect of hsa_circ_0007905 on the malignant phenotype of CSCs, we further studied the molecular mechanism of hsa_circ_0007905. The identification of hsa_circ_0007905 structure and location suggests that hsa_circ_0007905 may be involved in post-transcriptional regulation. Therefore, we predicted by ENCORI that hsa_circ_0007905 can bind to miR-330-5p (Fig. 3A), and further verified by dual luciferase reporter gene experiment (Fig. 3B). There was a notable reduction in the luciferase activity of the hsa_circ_0007905 WT vector after miR-330-5p mimics transfection. The RNA pull-down test revealed a notable rise in the enrichment of hsa_circ_0007905 in the Bio-miR-330-5p-WT group (Fig. 3C).

miR-330-5p expression in CC tissues decreased significantly compared to adjacent tissues, and it negatively correlated with hsa_circ_0007905 expression (Fig. 3D,E). In CC cell lines, miR-330-5p was lower compared with Ect1/E6E7 (Fig. 3F). miR-330-5p in CD133+ CaSki cells was downregulated compared with CaSki cells (Fig. 3G).

Hsa_circ_0007905 promotes stemness and inhibits apoptosis of CSCs by inhibiting miR-330-5p

Rescue experiments were designed to verify the role of miR-330-5p in the regulation of hsa_circ_0007905 on the malignant phenotype of CSCs. miR-330-5p inhibitors counteracted the inhibition of cell growth and the encouragement of apoptosis, which were mediated by hsa_circ_0007905 downregulation. As a result of downregulation of hsa_circ_0007905, Bax was up-regulated and Bcl-2 was down-regulated. However, the trend was blocked by inhibiting miR-330-5p (Fig. 4C). miR-330-5p inhibitors increased the number of sphere formation (Fig. 4D) and CD44, OCT4 and SOX2 protein expression (Fig. 4E). Down-regulating miR-330-5p impaired hsa_circ_0007905-driven suppression of cellular migratory and invasive activities (Fig. 4F,G).

VDAC1 is a target gene of miR-330-5p

The bioinformatics website predicted that miR-330-5p had a targeting relationship with VDAC1 (Fig. 5A). As dem-

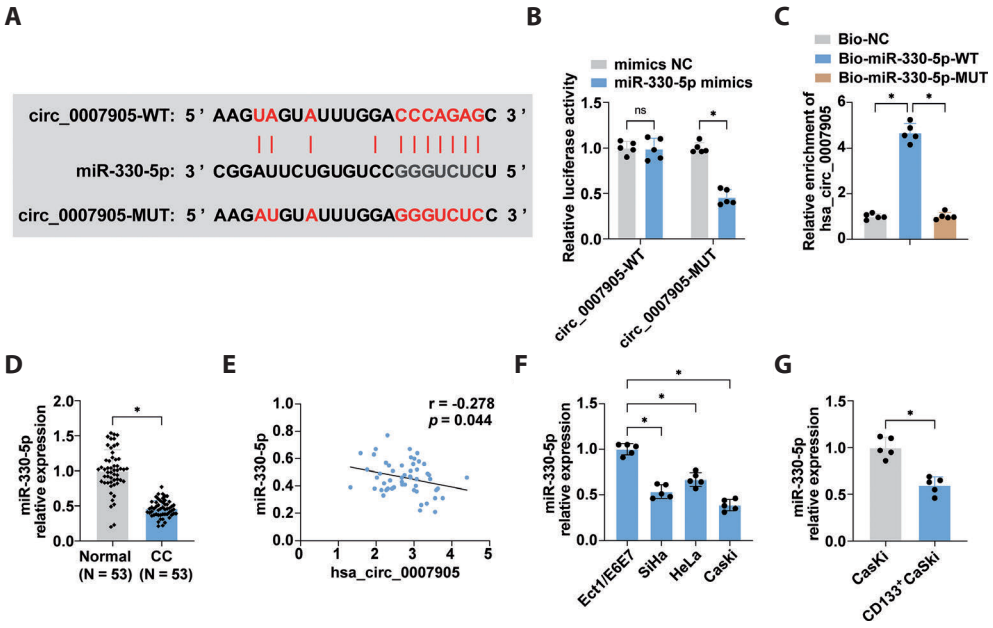

Figure 3. Hsa_circ_0007905 targets miR-330-5p. **A.** Schematic illustration of hsa_circ_0007905 wild-type (WT) and mutant (MUT) luciferase reporter vectors constructed according to the binding sites of hsa_circ_0007905 and miR-330-5p that predicted by bioinformatics website https://rnasysu.com/encori/index.php. **B.** Luciferase reporter gene assay to verify the binding relationship between hsa_circ_0007905 and miR-330-5p. **C.** RNA pull-down assay to verify the binding relationship between hsa_circ_0007905 and miR-330-5p. **D.** RT-qPCR to detect the expression of miR-330-5p in CC tissues and adjacent tissues (n = 53). **E.** Correlation analysis of hsa_circ_0007905 and miR-330-5p expression levels in CC tissues (n = 53). **F.** RT-qPCR to detect the expression of miR-330-5p in Ect1/E6E7 and human CC cell lines SiHa, HeLa and CaSki. **G.** RT-qPCR to detect miR-330-5p in CD133$^+$ CaSki cells and CaSki cells. * $p < 0.05$.

onstrated by the dual luciferase reporter gene assay, cells co-transfected with VDAC1-WT and miR-330-5p mimics had significant decreased relative luciferase activity (Fig. 5B). RNA pull-down experiments further verified this targeting relationship (Fig. 5C). VDAC1 expression in CC tissues notably exceeded that in adjacent tissues, showing an inverse relationship with miR-330-5p expression (Fig. 5D,E). VDAC1 protein in CC cell lines was also significantly higher than that in Ect1/E6E7 (Fig. 5F). The upregulation of VDAC1 was detected in CD133$^+$ CaSki cells compared with CaSki cells (Fig. 5G). Up-regulation of miR-330-5p could inhibit VDAC1 (Fig. 5H).

VDAC1 in CC tissues was positively correlated with hsa_circ_0007905 (Fig. 5I). After knocking down hsa_circ_0007905, VDAC1 expression was inhibited, and down-regulation of miR-330-5p could reverse this trend (Fig. 5H).

Overexpressing VDAC1 reduces the effect of silencing hsa_circ_0007905 on the malignant phenotype of CSCs

By transfecting pcDNA3.1-VDAC1, we successfully restored VDAC1 expression in CD133$^+$ CaSki cells with low expression of hsa_circ_0007905 (Fig. 6A). Increasing VDAC1 levels counteracted the suppression of cell growth and the promotion of cell apoptosis mediated by inhibiting hsa_circ_0007905 (Fig. 6B,C). After overexpression of VDAC1, Bax was down-regulated and Bcl-2 was up-regulated (Fig. 6D). CSC sphere formation ability may be restored through upregulation of VDAC1 to reverse the effects of silencing hsa_circ_0007905 (Fig. 6E). Similarly, up-regulation of VDAC1 significantly promoted the protein expression of CD44, OCT4 and SOX2 (Fig. 6F). Promoting VDAC1 reversed the inhibition of hsa_circ_0007905 on cell migration and invasion (Fig. 6G,H).

Discussion

CSCs are tumor cells with self-renewal and multi-directional differentiation potential. There is increasing evidence that CSCs have tumor-initiating ability and play a vital role in tumor metastasis, recurrence and chemotherapy/radiation resistance (Huang et al. 2020; Bayik and Lathia 2021). Elucidating the regulatory mechanism of CSC characteristics is helpful to further understand the molecular mechanism of malignant tumors, and then discover new molecular mark-

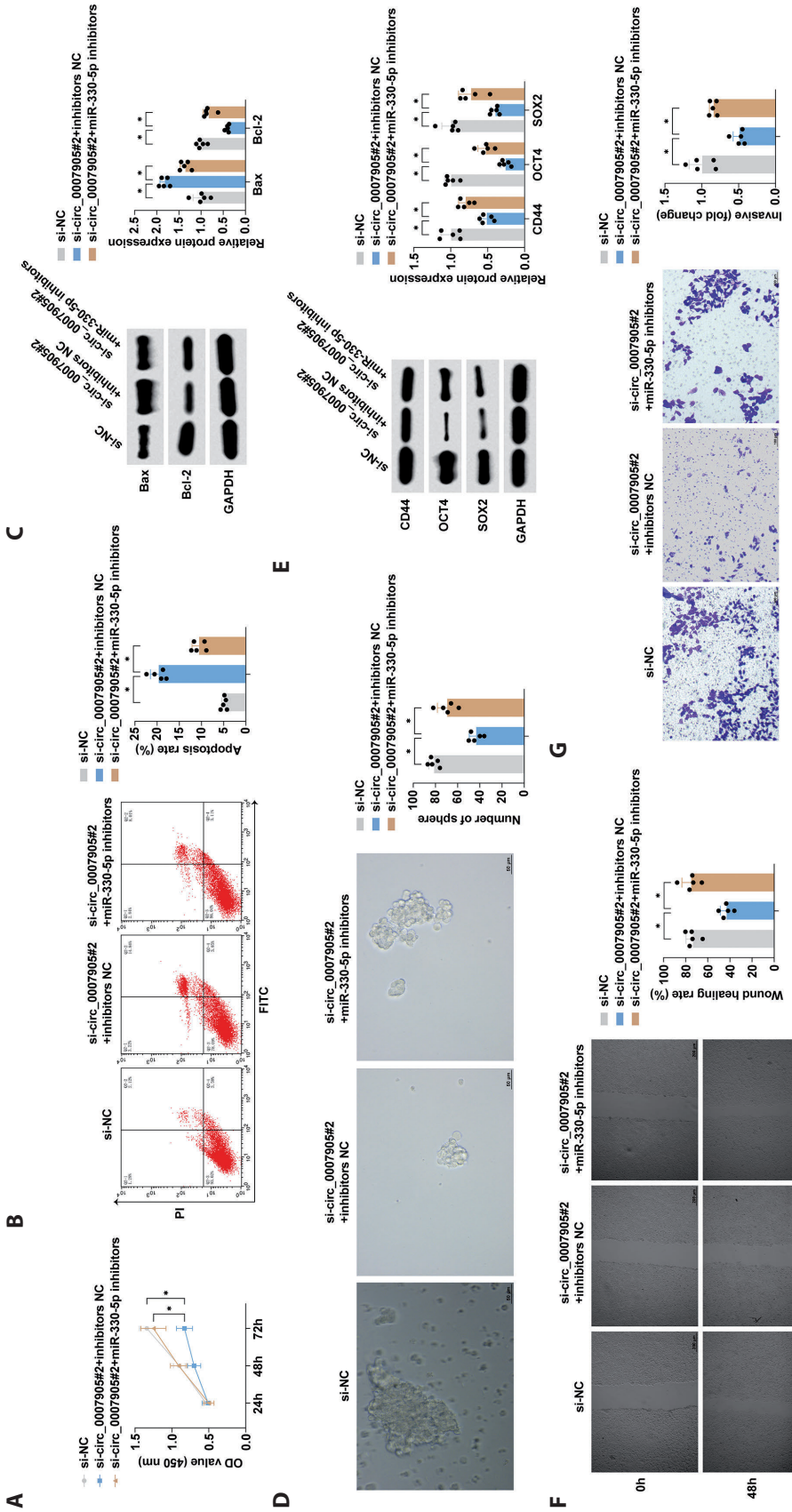

Figure 4. Hsa_circ_0007905 promotes CSC stemness and inhibits apoptosis by inhibiting miR-330-5p. **A.** CCK-8 assay to detect cell proliferation. **B.** Flow cytometry to detect apoptosis. **C.** Western blot to detect the protein expression of Bax and Bcl-2. **D.** Sphere formation assay to detect the number of spheres. **E.** Western blot to detect the protein expression of CD44, OCT4 and SOX2. **F.** Scratch test to detect cell migration in each group. **G.** Transwell to detect cell invasion. * $p < 0.05$.

ers and therapeutic targets. CD133 protein is widely used as a CSC marker in a variety of tumors. In CC cells, SP cells sorted by flow cytometry have higher expression of CD133 than non-SP cells, and have stem cell-like proliferation, differentiation, self-renewal, chemoradiotherapy resistance and tumorigenic ability. Therefore, CD133 may be a specific marker on the surface of CSCs, which can accurately identify stem cells (Ruixia and Einar 2016). In this study, we isolated CD133$^+$ CaSki cells from CaSki by flow cytometry, and CSC markers CD44, OCT4 and SOX2 levels were significantly increased, suggesting that CSCs were successfully isolated. Suppression of hsa_circ_0007905 significantly reduced the growth, self-renewal, migration, and invasion of CD133$^+$ CaSki cells, while enhancing apoptosis.

circRNAs as competitive endogenous RNA and miRNAs binding to reduce the ability of miRNAs to target mRNA is a classic molecular regulatory network. miRNAs destroy the stability of mRNA by specifically binding to the 3'UTR of the target gene and inhibit the translation of mRNA. There have been reports that miRNAs are abnormally expressed

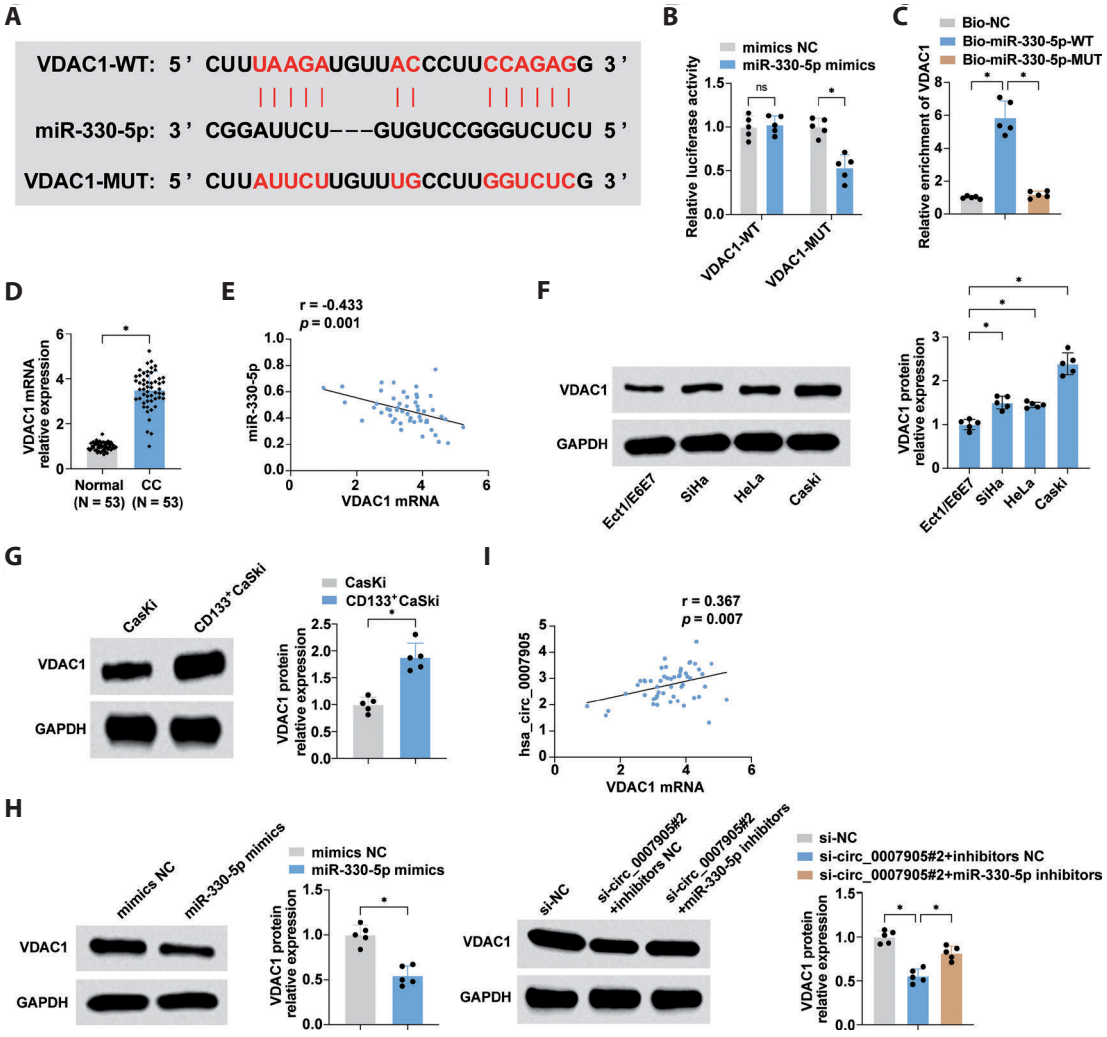

Figure 5. VDAC1 is a target gene of miR-330-5p and is indirectly regulated by hsa_circ_0007905. **A.** Schematic illustration of VDAC1 wild-type (WT) and mutant (MUT) luciferase reporter vectors constructed according to the binding sites of VDAC1 and miR-330-5p that predicted by bioinformatics website https://rnasysu.com/encori/index.php. **B.** Luciferase reporter gene assay to verify the targeted binding relationship between miR-330-5p and VDAC1. **C.** RNA pull-down assay to verify the targeted binding relationship between miR-330-5p and VDAC1. **D.** RT-qPCR to detect the expression of VDAC1 mRNA in CC tissues and adjacent tissues ($n = 53$). **E.** Correlation analysis of VDAC1 and miR-330-5p expression levels in CC tissues ($n = 53$). **F.** Western blot to detect the expression of VDAC1 in Ect1/E6E7 and human CC cell lines SiHa, HeLa and CaSki. **G.** Western blot to detect the expression of VDAC1 protein in CD133$^+$ CaSki cells and CasKi cells. **H.** Western blot to detect VDAC1 in CD133$^+$ CaSki after transfection. **I.** Correlation analysis of VDAC1 and hsa_circ_0007905 expression levels in CC tissues. * $p < 0.05$.

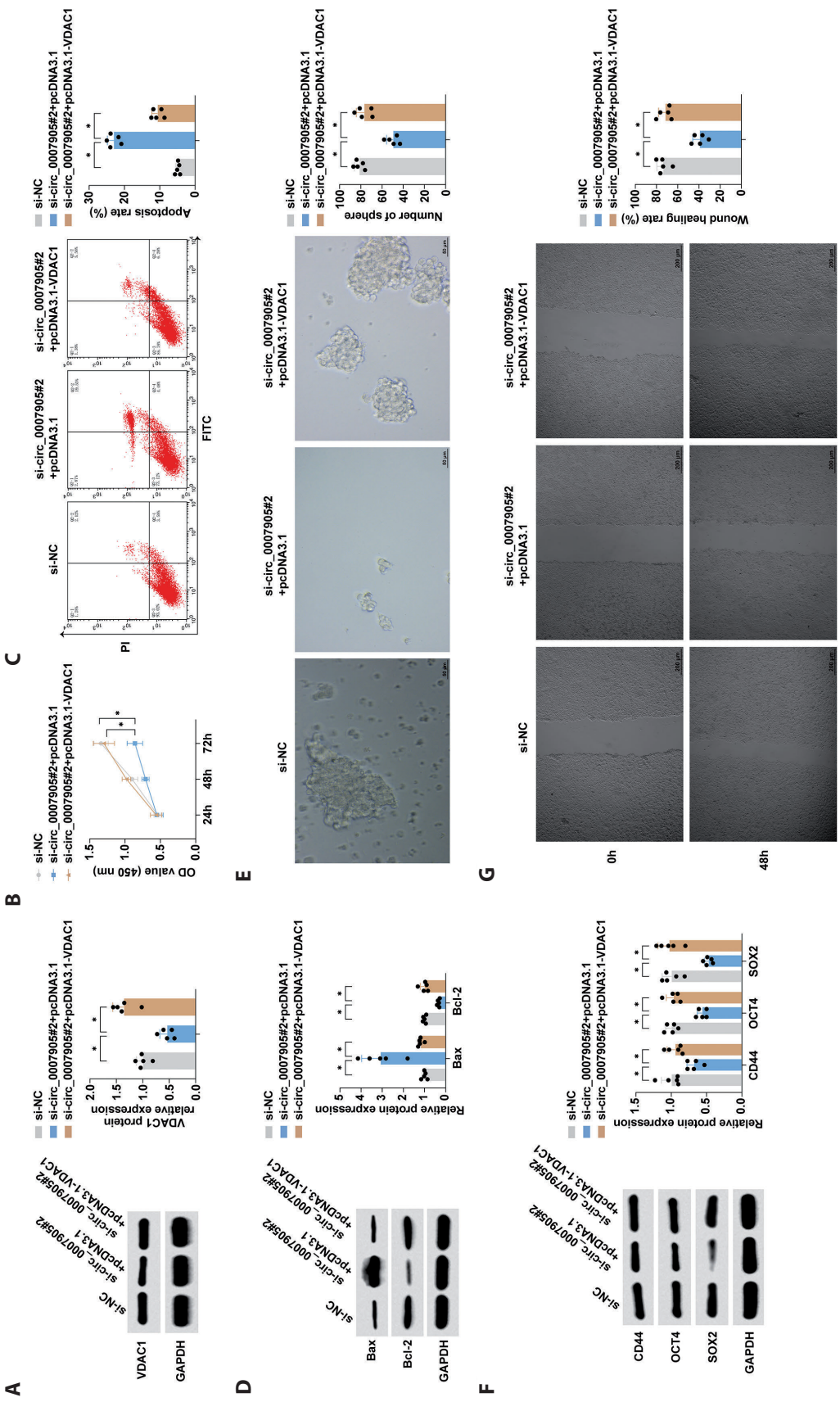
A
si-NC
si-circ_0007905#2+pcDNA3.1
si-circ_0007905#2+pcDNA3.1-VDAC1
VDAC1 protein relative expression
VDAC1
GAPDH
B
OD value (450 nm)
24h
48h
72h
C
si-NC
si-circ_0007905#2 +pcDNA3.1
si-circ_0007905#2 +pcDNA3.1-VDAC1
PI
FITC
Apoptosis rate (%)
D
Relative protein expression
Bax
Bcl-2
GAPDH
E
Number of sphere
F
CD44
OCT4
SOX2
G
0h
48h
Wound healing rate (%)

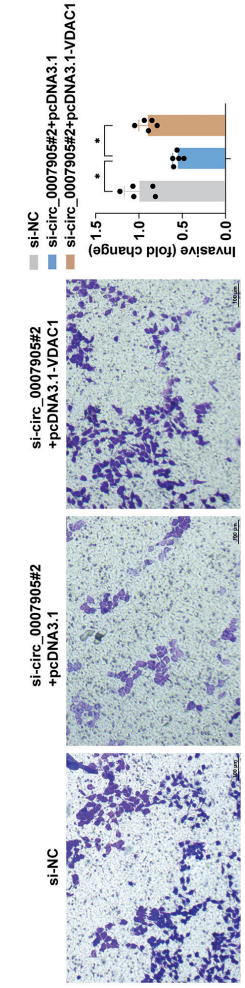

Figure 6. Overexpression of VDAC1 reverses the effect of silencing hsa_circ_0007905 on the malignant phenotype of CC stem cells. **A.** Western blot to detect VDAC1 in $CD133^+$ CaSki after transfection. **B.** CCK-8 assay to detect cell proliferation. **C.** Flow cytometry to detect apoptosis. **D.** Western blot to detect the protein expression of Bax and Bcl-2. **E.** Sphere formation assay to detect the number of spheres. **F.** Western blot to detect the protein expression of CD44, OCT4 and SOX2. **G.** Scratch test to detect cell migration in each group. **H.** Transwell to detect cell invasion. * $p < 0.05$.

in CC cells and regulate their proliferation, apoptosis and invasion (Shen et al. 2020). Our findings verify that miR-330-5p specifically bind to hsa_circ_0007905 and undergoes negative regulation by hsa_circ_0007905. Furthermore, there was a decrease in miR-330-5p levels in CC tissues and cells, aligning with its expression pattern in CC identified in an earlier research (Jafarzadeh et al. 2022). In an effort to elucidate miR-330-5p's function in controlling CSCs *via* hsa_circ_0007905, our rescue studies on $CD133^+$ CaSki cells revealed that reducing miR-330-5p significantly hindered CSC growth and self-renewal mediated by inhibiting hsa_circ_0007905, confirming the regulation of miR-330-5p by hsa_circ_0007905 in CSCs. miR-330-5p is regulated by the upstream regulator, long non-coding RNA, which affects miR-330-5p's effect on target genes, and impacting CC cells' malignant phenotype (Chen and Wang 2019; Zhou et al. 2020; Hou et al. 2022). hsa_circ_0007905 interacts with miR-330-5p in a manner that affects CSCs, and the downstream targets of miR-330-5p were explored further. Bioinformatics website prediction and mechanism research confirmed the targeted binding relationship between miR-330-5p and VDAC1 and VDAC1 was negatively regulated by miR-330-5p. VDAC1 is a pore egg located on the outer membrane of mitochondria, and its upregulation is strongly associated with poor prognoses (Wang et al. 2022). VDAC1 is also reported to be significantly up-regulated in CC and promotes CC development as a cancer-promoting factor (Zhang et al. 2019; Zhang et al. 2020). Finally, we also confirmed that hsa_circ_0007905 regulated the proliferation, apoptosis, migration, invasion and self-renewal of CSCs through VDAC1 through rescue experiments.

Conclusion

It can be concluded that hsa_circ_0007905 promotes the stemness of CSCs and inhibits apoptosis in CC by competitively adsorbing miR-330-5p to mediate VDAC1 expression. Our study provides new clues for further research on the mechanism of CC and the search for new therapeutic targets for CC.

Conflict of interest. The authors have no conflicts of interest to declare.

Availability of data and materials. The datasets used and/or analyzed during the present study are available from the corresponding author on reasonable request.

Ethics approval. The present study was approved by the Ethics Committee of Minda Hospital Affiliated to Hubei Minzu University (No. 2018ES0388) and written informed consent was provided by all patients prior to the study start. All procedures were performed in accordance with the ethical standards of the Institutional Review

Board and The Declaration of Helsinki, and its later amendments or comparable ethical standards.

Author's contribution. JZ designed the research study. JZ and YF performed the research. ChY provided help and advice. YF and ChY analyzed the data. JZ wrote the manuscript. ChY reviewed and edited the manuscript. All authors contributed to editorial changes in the manuscript. All authors read and approved the final manuscript.

References

Bayik D, Lathia J (2021): Cancer stem cell-immune cell crosstalk in tumour progression. Nat. Rev. Cancer **21,** 526-536 https://doi.org/10.1038/s41568-021-00366-w

Bray F, Ferlay J, Soerjomataram I, Siegel RL, Torre LA, Jemal A. (2018): Global cancer statistics 2018: GLOBOCAN estimates of incidence and mortality worldwide for 36 cancers in 185 countries. CA Cancer J. Clin. **68,** 394-424 https://doi.org/10.3322/caac.21492

Brisson M, Kim JJ, Canfell K, Drolet M, Gingras G, Burger EA, Martin D, Simms KT, Bénard É, Boily MC, et al. (2020): Impact of HPV vaccination and cervical screening on cervical cancer elimination: a comparative modelling analysis in 78 low-income and lower-middle-income countries. Lancet **395,** 575-590 https://doi.org/10.1016/S0140-6736(20)30068-4

Buskwofie A, David-West G, ClareCA (2020): A review of cervical cancer: Incidence and disparities. J. Natl. Med. Assoc. **112,** 229-232 https://doi.org/10.1016/j.jnma.2020.03.002

Chen L, Shan G (2021): CircRNA in cancer: Fundamental mechanism and clinical potential. Cancer Lett. **505,** 49-57 https://doi.org/10.1016/j.canlet.2021.02.004

Chen S, Wang J (2019): HAND2-AS1 inhibits invasion and metastasis of cervical cancer cells via microRNA-330-5p-mediated LDOC1. Cancer Cell Int. **19,** 353 https://doi.org/10.1186/s12935-019-1048-y

Chen S, Yang X, Yu C, Zhou W, Xia Q, Liu Y, Chen Q, Chen X, Lv Y, Lin Y (2021): The potential of circRNA as a novel diagnostic biomarker in cervical cancer. J. Oncol. **2021,** 5529486 https://doi.org/10.1155/2021/5529486

Di Fiore R, Suleiman S, Drago-Ferrante R, Subbannayya Y, Pentimalli F, Giordano A, Calleja-Agius J (2022): Cancer stem cells and their possible implications in cervical cancer: A short review. Int. J. Mol. Sci. **23,** 5167 https://doi.org/10.3390/ijms23095167

Ferrall L, Lin K, Roden R, Hung C, Wu T (2021): Cervical cancer immunotherapy: Facts and hopes. Clin. Cancer Res. **27,** 4953-4973 https://doi.org/10.1158/1078-0432.CCR-20-2833

Gao Z, Wang Q, Ji M, Guo X, Li L, Su X (2021): Exosomal lncRNA UCA1 modulates cervical cancer stem cell self-renewal and differentiation through microRNA-122-5p/SOX2 axis. J. Transl. Med. **19,** 229 https://doi.org/10.1186/s12967-021-02872-9

Guo M, Xu J, Du J. (2021): Trends in cervical cancer mortality in China from 1989 to 2018: an age-period-cohort study and Joinpoint analysis. BMC Public Health **21,** 1329 https://doi.org/10.1186/s12889-021-11401-8

Hou S, Zhang X, Yang J (2022): Long non-coding RNA ABHD11-AS1 facilitates the progression of cervical cancer by competitively binding to miR-330-5p and upregulating MARK2. Exp. Cell Res. **410,** 112929 https://doi.org/10.1016/j.yexcr.2021.112929

Huang T, Song X, Xu D, Tiek D, Goenka A, Wu B, Sastry N, Hu B, Cheng S (2020): Stem cell programs in cancer initiation, progression, and therapy resistance. Theranostics **10,** 8721-8743 https://doi.org/10.7150/thno.41648

Hyuna S, Jacques F, Rebecca L S, Mathieu L, Isabelle S, Ahmedin J, Freddie B (2021): Global cancer statistics 2020: GLOBOCAN estimates of incidence and mortality worldwide for 36 cancers in 185 countries. CA Cancer J. Clin. **71,** 209-249 https://doi.org/10.3322/caac.21660

Jafarzadeh A, Paknahad M, Nemati M, Jafarzadeh S, Mahjoubin-Tehran M, Rajabi A, Shojaie L, Mirzaei H (2022): Dysregulated expression and functions of microRNA-330 in cancers: A potential therapeutic target. Biomed. Pharmacother. **146,** 112600 https://doi.org/10.1016/j.biopha.2021.112600

Koh W, Abu-Rustum N, Bean S, Bradley K, Campos S, Cho K, Chon H, Chu C, Clark R, Cohn D et al. (2019): Cervical Cancer, Version 3.2019, NCCN Clinical Practice Guidelines in Oncology. J. Natl. Compr. Canc. Netw. **17,** 64-84 https://doi.org/10.6004/jnccn.2019.0001

Lu J, Ru J, Chen Y, Ling Z, Liu H, Ding B, Jiang Y, Ma J, Zhang D, Ge J et al. (2023): N -methyladenosine-modified circSTX6 promotes hepatocellular carcinoma progression by regulating the HNRNPD/ATF3 axis and encoding a 144 amino acid polypeptide. Clin. Transl. Med. **13,** e1451 https://doi.org/10.1002/ctm2.1451

Ma Y, Liu J, Yang Z, Chen P, Wang D (2022): CircRNA_400029 promotes the aggressive behaviors of cervical cancer by regulation of miR-1285-3p/TLN1 axis. J. Cancer **13,** 541-553 https://doi.org/10.7150/jca.61437

Mailinh V, Jim Y, Olutosin A A, Linus C (2018): Cervical cancer worldwide. Curr. Probl. Cancer **42,** 457-465 https://doi.org/10.1016/j.currproblcancer.2018.06.003

Meng L, Zhang Y, Wu P, Li D, Lu Y, Shen P, Yang T, Shi G, Chen Q, Yuan H et al. (2022): CircSTX6 promotes pancreatic ductal adenocarcinoma progression by sponging miR-449b-5p and interacting with CUL2. Mol. Cancer **21,** 121 https://doi.org/10.1186/s12943-022-01599-5

Qi W, Zhao C, Zhao L, Liu N, Li X, Yu W, Wei L (2014): Sorting and identification of side population cells in the human cervical cancer cell line HeLa. Cancer Cell Int. **14,** 3 https://doi.org/10.1186/1475-2867-14-3

Ruixia H, Einar KR (2016): Cancer stem cells (CSCs), cervical CSCs and targeted therapies. Oncotarget **8,** 35351-35367 https://doi.org/10.18632/oncotarget.10169

Shen S, Zhang S, Liu P, Wang J, Du H (2020): Potential role of microRNAs in the treatment and diagnosis of cervical cancer. Cancer Genet. 248-249, 25-30 https://doi.org/10.1016/j.cancergen.2020.09.003

Song T, Xu A, Zhang Z, Gao F, Zhao L, Chen X, Gao J, Kong X (2019): CircRNA hsa_circRNA_101996 increases cervical cancer proliferation and invasion through activating TPX2 expression by restraining miR-8075. J. Cell Physiol. **234,** 14296-14305

https://doi.org/10.1002/jcp.28128
Wang W, Li L, Wu M, Ma S, Tan X, Zhong S (2019): Laparoscopic vs. abdominal radical hysterectomy for locally advanced cervical cancer. Front. Oncol. **9,** 1331 https://doi.org/10.3389/fonc.2019.01331
Wang Z, Cheng Y, Song Z, Zhao R (2022): Pan-cancer analysis of voltage-dependent anion channel (VDAC1) as a cancer therapeutic target or diagnostic biomarker. Dis. Markers **2022,** 5946110 https://doi.org/10.1155/2022/5946110
Wei W, Liu K, Huang X, Tian S, Wang H, Zhang C, Ye J, Dong Y, An Z, Ma X et al. (2024): EIF4A3-mediated biogenesis of circSTX6 promotes bladder cancer metastasis and cisplatin resistance. J. Exp. Clin. Cancer Res. **43,** 2 https://doi.org/10.1186/s13046-023-02932-6
Yang M, Hu H, Wu S, Ding J, Yin B, Huang B, Li F, Guo X, Han L (2022): EIF4A3-regulated circ_0087429 can reverse EMT and inhibit the progression of cervical cancer via miR-5003-3p-dependent upregulation of OGN expression. J. Exp. Clin. Cancer Res. **41,** 165 https://doi.org/10.1186/s13046-022-02368-4
Yao T, Lu R, Zhang Y, Zhang Y, Zhao C, Lin R, Lin Z (2015): Cervical cancer stem cells. Cell Prolif. **48,** 611-625 https://doi.org/10.1111/cpr.12216
Zhang C, Hua Y, Qiu H, Liu T, Long Q, Liao W, Qiu J, Wang N, Chen M, Shi D et al. (2020): KMT2A regulates cervical cancer cell growth through targeting VDAC1. Aging **12,** 9604-9620 https://doi.org/10.18632/aging.103229
Zhang X, Zhao X, Li Y, Zhou Y, Zhang Z (2019): Long noncoding RNA SOX21-AS1 promotes cervical cancer progression by competitively sponging miR-7/VDAC1. J. Cell Physiol. **234,** 17494-17504 https://doi.org/10.1002/jcp.28371
Zhou Q, Xie Y, Wang L, Xu T, Gao Y (2020): LncRNA EWSAT1 upregulates CPEB4 via miR-330-5p to promote cervical cancer development. Mol. Cell Biochem. **471,** 177-188 https://doi.org/10.1007/s11010-020-03778-8

Received: August 27, 2024
Final version accepted: December 29, 2024